Low-Threshold Lasing and Coherent Perfect Absorption in Generalized PT-Symmetric Optical Structures

Maryam Sakhdari, Nasim Mohammadi Estakhri, Hakan Bagci, and Pai-Yen Chen

Low-Threshold Lasing and Coherent Perfect Absorption in the Generalized PT-Symmetric Optical Structures

Maryam Sakhdari[1], Nasim Mohammadi Estakhri[2], Hakan Bagci[3], and
Pai-Yen Chen[1,*]

[1]*Department of Electrical and Computer Engineering, Wayne State University, Detroit, MI 48017, U.S.A.*

[2]*Department of Electrical and Systems Engineering, University of Pennsylvania, Philadelphia, PA 19104, USA*

[3]*Computer, Electrical, and Mathematical Science and Engineering Division, King Abdullah University of Science and Technology (KAUST), Thuwal 23955-6900, Saudi Arabia*

RECEIVED DATE

Corresponding Author: Email: pychen@wayne.edu

ABSTRACT

Achieving exact balance between spatially separated gain and loss is generally regarded as a necessary condition for parity–time (PT)-symmetric optical systems [1]-[12]. We introduce generalized PT (gPT)-symmetric optical structures, which have an asymmetric and unbalanced gain-loss profile, while exhibiting similar scattering properties and phase transitions as their traditional PT-symmetric counterparts. In particular, we show that the concept of gPT-symmetry may help reducing the threshold gain in achieving newly discovered PT-enabled applications, such as the coherent perfect absorber (CPA)-laser and exceptional points. The concept proposed herein will facilitate the practice of PT-symmetric optical and photonic devices by offering greater design flexibility to tailor gain-loss profiles and their thresholds.

Introduction. Recently, parity-time (PT)-symmetric optics has attracted intense research interest, as it provides an experimentally-accessible platform to study real eigenspectra in physical systems with non-Hermitian Hamiltonians [1]-[12]. Optical systems satisfying PT-symmetry must consist of a lasing medium and its time-reversed lossy counterpart, of which gain and loss contributions are equally balanced and symmetrically distributed in space, e.g., an optical system with complex permittivities having a spatial profile of $\varepsilon(\mathbf{r}) = \varepsilon^*(-\mathbf{r})$ [1],[2] [see Fig. 1a]. During recent years, numerous intriguing optical phenomena and applications have been observed in PT-symmetric systems, including PT–symmetry phase transitions and exceptional points [1],[2], unidirectional reflectionless light propagation [3]-[5], negative refraction and sub-diffraction focusing [6], and optical isolators and circulators [7]. Particularly, a PT–symmetric optical system can behave simultaneously as a coherent perfect absorber (CPA) that fully absorbs incoming waves and a laser oscillator that emits outgoing coherent waves. Such an optical device is referred to as CPA-laser [8]-[12] because its exhibits both lasing and coherent perfect absorption modes at the same frequency, switchable via adjusting amplitudes and phases of incoming waves.

In this context, we have recently proposed a new generalized PT-symmetric electronic system, comprising the inductively coupled RLC tank (loss) and $-RLC$ tank (gain) [13]. In the electronic domain, we have demonstrated that with the newly introduced reciprocal scaling (X) operation that reciprocally scales charges stored in passive and active tanks, one can realize a PTX-symmetric system that shares the same eigenspectrum as its PT-symmetric counterparts, while, interestingly, having different circuit topologies, eigenmodes, and effective Q-factor (resonance linewidth) [13]. This finding motivates us to extend the reciprocally-scaling concept to the optical systems for breaking the balance between gain and loss coefficients, in order to gain more flexibility in design. In

this paper, we investigate a generalized PT (gPT)-symmetric optical system [Fig. 1b] with an unbalanced loss-gain profile, while displaying similar phase transitions and extraordinary scattering properties as those observed in a traditional PT-symmetric system. Quite contrary to typical PT-symmetric systems [Fig. 1a] characterized with balanced gain and loss, this gPT-symmetric system consists of the reciprocally scaled gain and loss parameters, i.e., $\kappa^2 \varepsilon(\mathbf{r})$ and $\varepsilon^*(-\mathbf{r})/\kappa^2$, with κ being a positive real coefficient. As detailed next, it is therefore possible that the loss parameter is greater than the gain parameter in the gPT-symmetric CPA-laser, with interesting similarities to the recently proposed concept of "loss-induced revival of lasing" [12],[14].

The concept of gPT-symmetric optical system. Figure 1a features a one-dimensional PT-symmetric optical system containing homogeneous, isotropic loss and gain media with permittivities $\varepsilon_{loss} = \varepsilon_r + i\varepsilon_i$ and $\varepsilon_{gain} = \varepsilon_{loss}^*$ [1]-[2]. Assuming a deeply subwavelength thickness for gain and loss media, i.e., $t_m \square \lambda$, this optical system can be described by a transmission-line model shown in Fig. 1a. The model consists of two admittance sheets with complex-valued surface admittances $Y_{s,loss} = Y_{s,r} + iY_{s,i} \approx -i\omega\varepsilon_{loss}t_m$ and $iY_{s,gain} = (iY_{s,loss})^*$ [15], where ω is the angular frequency. On the interface of each admittance sheet, electric fields are equal, $E_t^+ = E_t^-$, and tangential magnetic fields are discontinuous due to the induced surface current: $\hat{n} \times (H_t^+ - H_t^-) = E_t^+ Y_s$, where $\hat{n}$ is the unit normal vector of the surface. Gain and loss sheets are separated by a dielectric slab with thickness d and intrinsic material admittance $Y = \sqrt{\varepsilon/\varepsilon_0} Y_0$, where the admittance of the background medium $Y_0 = \sqrt{\mu_0/\varepsilon_0}$. In practice, such admittance sheets can also be realized with metasurfaces or two-dimensional nanomaterials [16]-[18], e.g. graphene under equilibrium (plasmon loss) [19]-[22] and population-inversion (plasmon gain) [23],[24]. Figure 1b illustrates the proposed gPT-symmetric optical system, where the surface admittance of the passive sheet and the admittance of its host substrate are scaled by the dimensionless scaling

factor κ, while those of the active sheet and its substrate are scaled by $1/\kappa$. To analyze scattering from the composite structure in Fig. 1, the electric field on left $(-)$ and right $(+)$ sides $E^{\pm} = E_f^{\pm} e^{ik^{\pm}z} + E_b^{\pm} e^{-ik^{\pm}z}$ are decomposed into forward- and backward-propagating waves, where their amplitudes are represented by $E_f^{\pm}$ and $E_b^{\pm}$ and $k^{\pm}$ are the wave numbers. $E_f^{\pm}$ and $E_b^{\pm}$ are related by:

$$\begin{pmatrix} E_f^+ \\ E_b^+ \end{pmatrix} = \mathbf{M} \begin{pmatrix} E_f^- \\ E_b^- \end{pmatrix}, \tag{1}$$

where $\mathbf{M}$ is the 2×2 transfer matrix. It can be readily shown that for both PT-symmetric and gPT-symmetric systems, $\det(\mathbf{M}) = 1$ for any κ, implying a reciprocal and unidirectional scattering [8]. In addition, $\mathbf{M}^* = \mathbf{M}^{-1}$ and $M_{22} = M_{11}^*$ are obtained in both systems. The transmission (t) and reflection (r) coe cients for left $(-)$ and right $(+)$ incidences can be expressed in terms of transfer matrix elements as $r^- = -M_{21}/M_{22}$, $r^+ = M_{12}/M_{22}$ and $t^+ = t^- = t = 1/M_{22}$. The scattering matrix linking incoming and outgoing waves is given by:

$$\mathbf{S} = \begin{pmatrix} t & r^+ \\ r^- & t \end{pmatrix} \text{ and } \begin{pmatrix} E_f^+ \\ E_b^- \end{pmatrix} = \mathbf{S} \begin{pmatrix} E_f^- \\ E_b^+ \end{pmatrix}. \tag{2}$$

The validity of PT-symmetry imposes a generalized conservation relation on the scattering matrix: $\mathbf{S}^*(\omega) = \mathcal{PT}\mathbf{S}(\omega)\mathcal{PT} = \mathbf{S}^{-1}(\omega)$ [9],[25], where the parity operator $\mathcal{P} = \begin{pmatrix} 0 & 1 \\ 1 & 0 \end{pmatrix}$, the time-reversal operator $\mathcal{T} = \begin{pmatrix} 0 & 1 \\ 1 & 0 \end{pmatrix}\mathcal{K}$, and $\mathcal{K}$ is the complex conjugation operator. For the gPT-symmetric system in Fig. 1b, scattering coefficients in $\mathbf{S}$ are derived using the transfer-matrix method as:

$$t^+ = t^- = \frac{i2\kappa YY_0 \csc(x)}{\kappa\left[Y^2 + (Y_0 + iY_{s,i})^2 - Y_{s,r}\right] + Y\left[Y_{s,i}(\kappa^2+1) + i\left(Y_0(\kappa^2+1) + Y_{s,r}(\kappa^2-1)\right)\right]\cot(x)};$$

$$r^+ = \frac{(1 + Y_{s,r}^2 + 2Y_{s,r} + Y_{s,i}^2 - s^2)\kappa - s\left[i(Y_{s,r}+1)(\kappa^2-1) + Y_{s,i}(\kappa^2+1)\right]\cot(x)}{\kappa\left[Y^2 + (Y_0+iY_{s,i})^2 - Y_{s,r}\right] + Y\left[Y_{s,i}(\kappa^2+1) + i\left(Y_0(\kappa^2+1) + Y_{s,r}(\kappa^2-1)\right)\right]\cot(x)}; \quad (3)$$

$$r^- = \frac{(1 + Y_{s,r}^2 + 2Y_{s,r} + Y_{s,i}^2 - s^2)\kappa - s\left[i(Y_{s,r}-1)(\kappa^2-1) + Y_{s,i}(\kappa^2+1)\right]\cot(x)}{\kappa\left[Y^2 + (Y_0+iY_{s,i})^2 - Y_{s,r}\right] + Y\left[Y_{s,i}(\kappa^2+1) + i\left(Y_0(\kappa^2+1) + Y_{s,r}(\kappa^2-1)\right)\right]\cot(x)},$$

where the electrical length between two admittance sheets $x=kd$.

Equation (3) reveals an interesting property of our gPT-symmetric system: if $x=(2n-1)\pi/2$, with n being a positive integer, all scattering coefficients of this generalized system become independent of κ, and they are therefore identical to those of the PT-symmetric setup in Fig. 1a, given by:

$$t^+ = t^- = \frac{i2YY_0}{Y_0^2 + Y^2 - 2iY_0Y_{s,i} - Y_{s,i}^2 - Y_{s,r}^2};$$

$$r^+ = \frac{Y_0^2 - Y^2 + (Y_{s,r} + Y_{s,i})^2}{Y_0^2 + Y^2 - 2iY_0Y_{s,i} - Y_{s,i}^2 - Y_{s,r}^2}; \quad (4)$$

$$r^- = \frac{Y_0^2 - Y^2 + (Y_{s,r} - Y_{s,i})^2}{Y_0^2 + Y^2 - 2iY_0Y_{s,i} - Y_{s,i}^2 - Y_{s,r}^2}.$$

In this case, PT- and gPT-symmetric optical systems share exactly the same **S** and **M**, and, therefore, our gPT-symmetric configuration, although having "unbalanced"gain and loss profiles, can achieve similar optical scattering properties enabled by PT-symmetry. As a result, the optical structure in Fig. 1b can be considered as a "generalized" PT-symmetric system with the traditional PT-symmetric system in Fig. 1a being a degenerate case of the gPT-symmetric system with $\kappa=1$. Since PT- and gPT-symmetric systems share the same **S** and its two eigenvalues $\lambda_{1,2}$, the transition between the *symmetry* and *symmetry-breaking* phases, typical for PT-symmetric scatters, can also be found in the gPT-symmetric system. The phase transition can be characterized by the evolution of eigenvalues given by [25]: $\lambda_{\pm} = t \pm \sqrt{r^- r^+} = t\left(1 \pm i\sqrt{1/|t|^2 - 1}\right)$. In the symmetry phase, the two eigenvalues are nondegenerate and unimodular (i.e., $|\lambda_{\pm}|=1$) and

5

$|t|<1.$ In the broken-symmetry phase, they are non-unimodular (i.e., $\lambda_+ = 1/(\lambda_-)^*$) and $|t|>1,$ with a transition point called exceptional point where $\lambda_+ = \lambda_- = 1/(\lambda_+)^*$ and $|t|=1.$ The lasing mode does occur in the symmetry-breaking phase of PT- and gPT-symmetric systems with $|t|>1,$ since the asymmetric **S** and eigenmodes could trap the excitation for a longer time in the gain part of the medium, rather than in the loss part [9].

A laser oscillator is an optical device that can provide output fields $E_b^-, E_f^+ \neq 0,$ even though input fields $E_f^-, E_b^+ \approx 0.$ The coherent perfect absorption mode would, on the other hand, require that $E_b^- = E_f^+ = 0$ and $E_f^-, E_b^+ \neq 0$ (i.e., the absence of reflected waves). Hence, a laser is developed if $M_{22} = 0$ and a CPA is developed if $M_{11} = 0$ and $E_b^+ / E_f^- = M_{21}.$ These two conditions, in general, do not occur simultaneously at the same frequency in the same system, but may be possible with the PT- and gPT-symmetric systems that allow $M_{22} = M_{11}^* = 0$ at the design frequency. The occurrence of CPA and laser has recently been theoretically studied [8],[9] and experimentally demonstrated [10],[11]. These two phenomena can be characterized by the overall output coefficient Θ, defined as the ratio of the total intensity of outgoing (reflected/transmitted) waves to that of the incoming waves [8]:

$$\Theta = \frac{|E_b^-|^2 + |E_f^+|^2}{|E_f^-|^2 + |E_b^+|^2} = \frac{\left|1 + M_{12}\alpha\right|^2 + \left|\alpha - M_{21}\right|^2}{\left(1 + |\alpha|^2\right)|M_{22}|^2}, \tag{5}$$

where $\alpha = E_b^+ / E_f^-.$ We should emphasize that for $\alpha = M_{21},$ which makes Θ zero, a CPA can be realized. On the other hand, for $\alpha \neq M_{21}$ (e.g. $\alpha = 0$ when considering only left-incident wave), the lasing mode is always obtained [8].

For the PT-symmetric surfaces in Fig. 1a, the CPA-laser can be attained in its symmetry-breaking phase, with a surface admittance profile:

$$Y_{s,loss} = Y_{s,r} + iY_{s,i} = Y_0 \sqrt{1 + (Y\csc(x)/Y_0)^2} + iY\cot(x); \tag{6a}$$

$$Y_{s,gain} = -Y_{s,r} + iY_{s,i}, \tag{6b}$$

which leads to $M_{22} = M_{11}^* = 0$. At the CPA-laser point, two eigenvalues of **S** become zero and infinity, which respectively correspond to the CPA and lasing modes [9]. The CPA-laser can be similarly achieved in our gPT-symmetric system, with the following generalized conditions:

$$Y_{s,loss} = \kappa Y_0 \sqrt{1 + Y^2 / Y_0^2} \, ; \tag{7a}$$

$$\text{and } Y_{s,gain} = -\kappa^{-1} Y_0 \sqrt{1 + Y^2 / Y_0^2} \, , \tag{7b}$$

where κ is the scaling factor that can be any arbitrary positive real number. We note that in the gPT-symmetric system, two surface admittances must be purely real to satisfy the CPA-laser condition. However, except for the special case of $\kappa = 1$, gain and loss are not necessarily equally balanced. Indeed, even if low-resonant gain and high-loss media are paired together (i.e. $\kappa \Box 1$ yielding $-\text{Re}[Y_{s,gain}] < \text{Re}[Y_{s,loss}]$), the CPA-laser point can still be attained. As a result, a low-threshold laser may be realized with a large κ, which makes $\Theta \rightarrow \infty$ provided that $\alpha \neq M_{21}$. Likewise, a small κ, yielding a system with high-gain and low-loss media, can interestingly achieve coherent perfect absorption with $\Theta \rightarrow 0$ provided that $\alpha = M_{21}$.

Implementations of generalized PT-symmetric CPA-laser. Next, we illustrate the gPT-symmetric system by examples of dispersive gain media with Lorentzian line shape, whose complex-valued permittivity can be expressed as [26]:

$$\varepsilon_{gain}(\omega) = \varepsilon_0 - \frac{\omega_p^2}{\omega_0^2 - \omega^2 + i\omega\gamma}, \tag{8}$$

where $\omega_p = 2\omega_0$ is the angular plasma frequency, ω_0 is the angular resonance frequency, and γ is the linewidth of amplification governing the magnitude of resonance. Note that the resonant gain decreases with increasing γ, and in order to satisfy the Kramers-Kronig relation and causality, γ of an active medium must be positive [26]. Further, a thin sheet of such a medium can be described by a surface conductivity $\sigma_{s,gain}(\omega) \approx -i\omega\varepsilon_{gain}(\omega)t_m$, equivalent to a surface admittance $Y_{s,gain} = \sigma_{s,gain}$. At the design frequency ω_D (wavelength λ_D) of the gPT-symmetric

CPA-laser, the amplifying and attenuating sheets are separated by a medium, with admittance $Y=Y_0$ and electrical length $x = \pi/2$. To satisfy the CPA-laser condition, $Y_{s,gain}(\omega_D) = -\sqrt{2}Y_0/\kappa$, as described in Eq. (7), this Lorentzian gain media must be patterned into proper metasurface structures. One possible structure can be an array of subwavelength strips with periodicity p and gap g [Fig. 1], whose equivalent surface admittance has an explicit form [Appendix]. The attenuating surface is assumed to be a resistive thin slab with constant conductivity (e.g. metals in the long wavelength region), resulting in $Y_{s,loss}(\omega_D) = \sqrt{2}Y_0\kappa$. Also, the host substrates for attenuating and amplifying sheets have a permittivity profile: $\varepsilon_1 = \kappa^2\varepsilon_0$ and $\varepsilon_2 = 1/\kappa^2\varepsilon_0$, which respectively render material admittances κY_0 and Y_0/κ, as shown in Fig. 1b. For simplicity, we assume that both host substrates are lossless and non-dispersive. However, our theoretical results (not presented here) show that around the design frequency, the CPA-laser mode is robust to moderate substrate losses.

The gain media in Fig. 2a with $\gamma = 0.198\omega_0$, $0.396\omega_0$, and $1.99\omega_0$, are utilized to realize gPT-symmetric CPA-laser devices with scaling factors $\kappa = 1/2$, 1, and 5, respectively, at the design frequency $\omega_D = 0.962\omega_0$. Figure 2b shows the transmittance $T = |t|^2$ versus the normalized frequency for different gPT-symmetric CPA-laser devices [Fig. 1b], illuminated by a single excitation ($\alpha \neq M_{21}$). For all devices, the thickness and gap-to-period ratio of metasurface $t_m = 0.004\,\lambda_D$ and $g/p = 0.08$, while the optimal period p is calculated using the explicit formula to achieve the CPA-laser mode [Appendix]. For example, if $\kappa = 5$, the active metasurface with $Y_{s,gain}(\omega_D) = -\sqrt{2}Y_0/\kappa$ is placed on the substrate with $\varepsilon_2 = \varepsilon_0/25$ (i.e., epsilon-near-zero (ENZ) material [27]), whereas the lossy sheet with $Y_{s,loss}(\omega_D) = \sqrt{2}Y_0\kappa$ is on a substrate with $\varepsilon_1 = 25\varepsilon_0$. From Fig. 2b, we find that regardless of γ, a lasing peak with a very large transmittance/reflectance is always achieved at ω_D, implying that there is, in

principle, no lasing threshold, namely lasing could happen even with a poor gain medium of large γ. Figure 2b also compares analytical results (lines) with those obtained using the (full-wave) finite-element method (dots) [28] and shows the good agreements around ω_D. The inset of Fig. 2b shows the magnitudes of λ_+ and λ_-, which respectively approach infinity and zero at ω_D, typical of a CPA-laser. To better understand this phenomenon, Fig. 3a presents transmittance T as function of κ and γ for our gPT-symmetric device under a single monochromatic excitation with frequency of ω_D. Again, for each value of κ, permittivities of host substrates are changed accordingly and the period of the active metasurface is optimized to achieve the maximum transmittance/reflectance. From Fig. 3a, it is seen that for any arbitrary γ, the lasing mode can always be found by choosing a proper κ. Moreover, peaks of transmittance are consistent with the locus of optimal sets of κ and γ (white dashed line) that represent $Y_{s,gain}(\omega_D) = -\sqrt{2}Y_0 / \kappa$.

Next, we study lasing behavior of an individual active metasurface and a traditional PT-symmetric CPA-laser, to make a fair comparison with the gPT-symmetric CPA-laser. Fig. 3b presents transmittance, while considering only the amplifying sheet, as shown in the inset. In this case, one side of the active metasurface is air and the other side is a dielectric substrate with permittivity $\varepsilon = \varepsilon_0 / \kappa^2$. The lasing mode with infinite reflectance/transmittance then occurs for $Y_{s,gain} = -(1+\sqrt{\varepsilon/\varepsilon_0})Y_0 = -(1+\kappa^{-1})Y_0$, exhibiting an physical bound: $Y_{s,gain}\big|_{\kappa\to\infty} \square -Y_0$, possible with an ENZ substrate that has a large κ. As can be seen in Fig. 3b, and in sharp contrast to the gPT-symmetric metasurface, it is not always possible to attain the lasing mode for values of γ beyond the threshold $\gamma_{th} = 0.56\,\omega_0$, which corresponds to $\text{Re}[\sigma_{gain}(\omega_D, \gamma_{th})] = -Y_0$. We note that for an active medium described by Eq. (8), the resonant gain ($-\text{Im}[\varepsilon_{gain}(\omega_D)]$ or $-\text{Re}[\sigma_{gain}(\omega_D)]$) decreases with increasing γ. Further, for the metasurface configuration in Fig. 1, the real part of the surface impedance has a tailorable

9

range: $0 < \mathrm{Re}[Y_{s,gain}] / \mathrm{Re}[\sigma_{s,gain}] \leq 1$, which depends on the area ratio of air to active medium [Appendix]. Consequently, for a weakly-resonant gain medium with $\gamma > \gamma_{th}$, $\mathrm{Re}[Y_{s,gain}(\omega_D)]$ is always out of the physical bound of lasing condition (i.e, $\mathrm{Re}[Y_{s,gain}(\omega_D)] > -Y_0$), which prohibits the lasing effect, as observed in Fig. 3b.

Here, we also consider the PT-symmetric system in Fig. 1a, with $iY_{s,loss} = (iY_{s,gain})^*$, but with an intermediary medium with $\varepsilon = \varepsilon_0 / \kappa^2$ and $x = (k_0 / \kappa)d$. Figure 3c presents contours of T as functions of γ and κ for this PT-symmetric system, under a single monochromatic excitation with frequency of ω_D; the left, middle and right panels show results for $\kappa = 1$, $1/2$ and 5, respectively, and for each set of κ and x, the active metasurface is optimized by fixing g / p to 0.08 and sweeping p to reach the maximum transmittance/reflectance. As can be seen in Fig. 3c, although it is possible to attain the CPA-laser mode in such a system, a finite γ_{th} exists for the lasing and CPA modes. Although a large κ and a suitable electrical length $x = (2n-1)\pi / 2$, leading to a CPA-laser condition of $Y_{s,r} = -Y_0 \sqrt{1 + (Y \csc(x) / Y_0)^2} \sim -Y_0$ and $Y_{s,i} = -Y_0 Y \cot(x) / Y_0 \sim 0$, may help increase γ_{th}, the maximum γ_{th} cannot be greater than $0.56 \omega_0$, analogous to that of an individual amplifying metasurface. Figure 3a also compares optimum γ versus κ at the lasing point ω_D for the single metasurface amplifier (blue dashed line) [Fig. 3b], PT-symmetric metasurface with $x = \pi / 2$ (green dashed line) [Fig. 3c], and the gPT-symmetric metasurface [Fig. 3a]. It is evident that if the active metasurface is made of a weakly-resonant gain (sheet) medium of a large γ, the lasing effect is only achievable in the gPT-symmetric system that essentially has no gain threshold.

Finally, we study the CPA mode of gPT-symmetric composite structures in Fig. 2b. Figure 4a shows their output coefficient Θ versus frequency; here, the solid lines represent the one-sided illumination with $\alpha = 0$ (which leads to the lasing

mode) and the dashed lines represent the doubled-sided illuminations with $\alpha = M_{21}$. For all three cases, $M_{21} = i\,(-1+\sqrt{2})$ at ω_D. It can be seen from Fig. 4a that the CPA and lasing can be obtained at the same frequency by simply switching the amplitude and phase of the second incoming signal. We should note that variations in transmittance/reflectance (i.e., modulation depth) of gPT-symmetric CPA-laser can be quite dramatic, which is ideal for optical switching and modulation applications. Figure 4b presents the full-wave simulation results for the CPA (top panel) and lasing (bottom panel) effects at ω_D, showing that the outgoing wave can be either fully suppressed or amplified, depending on how the coherent signal is tuned. Again, there is no threshold gain for our gPT-symmetric CPA.

Conclusion. Controlling the balance between gain and loss is typically regarded as the necessary condition to realize a PT-symmetric classical wave system. Here, we have introduced the idea of a generalized PT-symmetric system with unbalanced, reciprocally-scaled gain and loss parameters, which interestingly possesses similar scattering properties and eigenvalue bifurcations as typical PT-symmetric systems. Specifically, we have demonstrated this idea using the PT-symmetric metasurfaces and shown that the CPA-laser mode can be realized even though the system has an unbalanced gain-loss profiles. Our results may provide new directions for advances in PT-symmetry and its electromagnetic, acoustic, and circuit applications via breaking the parametric balance between gain and loss and eradicating the threshold gain/loss for reaching exotic properties of PT-symmetry, such as the and CPA-laser mode and exceptional points.

Appendix: metasurface designs. According to impedance boundary conditions, a discontinuity on the tangential magnetic field on the metasurface is related to the induced averaged surface current by the surface admittance. Assuming perfectly-conducting strips of negligible thickness are aligned parallel to the magnetic field

of the transverse magnetic (TM) incident wave, the equivalent surface admittance can be explicitly written as [15],[29],[30]:

$$Y_s = -i2\alpha Y_{eff},\tag{A1}$$

and
$$\alpha = \frac{k_{eff}\,p}{\pi}\left[\ln\left(\csc\left(\frac{\pi g}{2p}\right)\right)+\frac{1}{2}\sum_{n=-\infty,n\neq 0}^{\infty}\left(\frac{2\pi}{\sqrt{(2\pi n)^2 - k_{eff}^2 p^2}}\frac{1}{|n|}\right)\right]$$

$$\approx \frac{k_{eff}\,p}{\pi}\ln\left(\csc\left(\frac{\pi g}{2p}\right)\right) \quad\text{if}\quad k_{eff}\,p\ \Box\ 2\pi\tag{A2}$$

where $Y_{eff} = \sqrt{\varepsilon_{eff}/\mu_0}$, $k_{eff} = \omega\sqrt{\mu_0\varepsilon_{eff}}$, $\varepsilon_{eff} = (\varepsilon+\varepsilon_0)/2$. When a dispersive medium is used to constitute the metasurface, the surface admittance is usually complex-valued, $Y_s = Y_{s,r} + iY_{s,i}$, where the surface conductance $Y_{s,r}$ and the surface susceptance $Y_{s,i}$ account for the gain/loss magnitude and the net stored energy in the near field, respectively. When considering a complex-valued sheet conductivity, the surface impedance of metasurface should be modified as [15]:

$$Y_s = \left[\frac{1}{\sigma_s(1-g/p)}+i\frac{1}{2\alpha Y_{eff}}\right]^{-1}.\tag{A3}$$

The scattering coefficients for an individual metasurface, placed on the interface between the left-sided background medium with admittance Y_0 and the right-sided medium with admittance Y, are given by:

$$r^- = \frac{Y_0 - Y - Y_{s,gain}}{Y + Y_0 + Y_{s,gain}},\quad r^+ = \frac{Y - Y_0 - Y_{s,gain}}{Y + Y_0 + Y_{s,gain}},$$

$$t^+ = \sqrt{Y_0/Y}(1+r^+),\, t^- = \sqrt{Y/Y_0}(1+r^-),\quad\text{and}\quad t^+ = t^-.\tag{A4}$$

The lasing condition that achieves transmittance/reflectance peaks can be derived as:

$$Y_{s,gain} = -(Y_0 + Y).\tag{A5}$$

In this case, the CPA effect can be obtained in a symmetric optical setup with $Y = Y_0$ and $E_f^- = E_b^+$, and the condition that makes $\Theta = 0$ can be derived as:

$$Y_{s,gain} = 2Y_0.\tag{A6}$$

From (A5) and (A6), it can be readily understood that CPA and laser do not simultaneously exist at a fixed frequency.

REFERENCES

[1] K. G. Makris, R. El-Ganainy, and D. N. Christodoulides, Beam Dynamics in PT Symmetric Optical Lattices, *Phys. Rev. Lett.* **100**, 103904 (2008).

[2] R. El-Ganainy, K. G. Makris, D. N. Christodoulides, and Z. H. Musslimani, Theory of Coupled Optical PT-Symmetric Structures, *Opt. Lett.* **32**, 2632-2634 (2007).

[3] Z. Lin, H. Ramezani, T. Eichelkraut, T. Kottos, H. Cao, and D. N. Christodoulides, "Unidirectional invisibility induced by PT-symmetric periodic structures." *Phys. Rev. Lett.* **106**, 213901 (2011).

[4] H. Ramezani, T. Kottos, R. El-Ganainy, and D. N. Christodoulides, Unidirectional Nonlinear PT –Symmetric Optical Structures, *Phys. Rev. A.* **82**, 043803 (2010).

[5] R. Fleury, D. L. Sounas, and A. Alù, "An invisible acoustic sensor based on parity-time symmetry," *Nat. Communications* **6**, 5905 (2015).

[6] R. Fleury, D. L. Sounas, and A. Alù, "Negative refraction and planar focusing based on parity-time symmetric metasurfaces," *Phys. Rev. Lett.* **113**, 023903 (2014).

[7] B. Peng, Ş. K. Özdemir, F. Lei, F. Monifi, M. Gianfreda, G. L. Long, S. Fan, F. Nori, C. M. Bender, and L. Yang, Parity-Time-Symmetric Whispering-Gallery Microcavities, *Nat. Phys*. **10**, 394 (2014).

[8] S. Longhi, PT -Symmetric Laser Absorber, *Phys. Rev. A* **82**, 031801(R) (2010).

[9] Y. D. Chong, L. Ge, and A. D. Stone, "PT-Symmetry Breaking and Laser-Absorber Modes in Optical Scattering Systems," *Phys. Rev. Lett*. **106**, 093902 (2011).

[10] Y. Sun, W. Tan, H. Q. Li, J. Li, and H. Chen, "Experimental demonstration of a coherent perfect absorber with PT phase transition," *Phys. Rev. Lett.*, **112**, 143903 (2014).

[11]   Z. J. Wong, Y. L. Xu, J. Kim, K. O'Brien, Y. Wang, L. Feng, and X. Zhang, "Lasing and anti-lasing in a single cavity," *Nat. Photon*. **10**, 796-801 (2016).

[12]   B. Peng, S. K. Özdemir, S. Rotter, H. Yilmaz, M. Liertzer, F. Monifi, C. M. Bender, F. Nori, and L. Yang, "Loss-induced suppression and revival of lasing." *Science* **346**, 328-332 (2014).

[13]   P. Y. Chen, M. Sakhdari, M. Hajizadegan, Q. Cui, M. Cheng, R. El-Ganainy, and A. A. Alù, "Generalized parity-time symmetry condition for enhanced sensor telemetry," *Nature Electronics*, in press (2018).

[14]   X. Lin, et al. "Loss induced amplification of graphene plasmons," *Opt. Lett.* **41**, 681-684 (2016).

[15]   S. Tretyakov, *Analytical modeling in applied electromagnetics*, Artech House, London (2003).

[16]   P. Y. Chen, M. Farhat, H. Bağcı, "Graphene metascreen for designing compact infrared absorbers with enhanced bandwidth," *Nanotechnol.* **26**, 164002 (2015).

[17]   P. Y. Chen, and A. Alù, "Terahertz metamaterial devices based on graphene nanostructures," IEEE Trans. Terahertz Sci. Technol. **3**, 748-756 (2013).

[18]   P. Y. Chen, and J. Jung, *PT*-Symmetry and Singularity-Enhanced Sensing Based on Photoexcited Graphene Metasurfaces. *Phys. Rev. Appl.* **5**, 064018 (2016).

[19]   P. Y. Chen, and A. Alù, "Atomically thin surface cloak using graphene monolayers," *ACS Nano* **5**, 5855-5863 (2011).

[20]   X. Lin, N. Rivera, J. J. López, I. Kaminer, H. Chen, and M. Soljačić, "Tailoring the energy distribution and loss of 2D plasmons," *N. J. Phys.* **18**, 105007 (2016).

[21]   X. Lin, et al. "All-angle negative refraction of highly squeezed plasmon and phonon polaritons in graphene–boron nitride heterostructures," Proc. Natl. Acad. Sci. 201701830 (2017).

[22]   X. Lin et al. "Splashing transients of 2D plasmons launched by swift electrons," *Science Advances* **3**, e1601192 (2017).

[23]   T. Watanabe, et al. "The gain enhancement effect of surface plasmon polaritons on terahertz stimulated emission in optically pumped monolayer graphene," *New J. Phys.* **15**, 075003 (2013).

[24]   D. Svintsov, V. Ryzhii, A. Satou, T. Otsuji, and V. Vyurkov, Carrier-Carrier Scattering and Negative Dynamic Conductivity in Pumped Graphene, *Opt. Express* **22**, 19873 (2014).

[25]   L. Ge, Y. D. Chong, and A. D. Stone, Conservation Relations and Anisotropic Transmission Resonances in One-Dimensional PT-Symmetric Photonic Heterostructures, *Phys. Rev. A* **85**, 023802 (2012).

[26]   A. A. Zyablovsky, A. P. Vinogradov, A. V. Dorofeenko, A. A. Pukhov, and A. A. Lisyansky, "Causality and phase transitions in PT-symmetric optical systems," *Phys. Rev. A* **89**, 033808 (2014).

[27]   I. Liberal, and N. Engheta, "Near-zero refractive index photonics," *Nat. Photonics* **11**, 149–158 (2017).

[28]   COMSOL Multiphysics: http://www.comsol.com.

[29]   Y. R. Padooru, A. B. Yakovlev, P. Y. Chen, and A. Alù, "Analytical modeling of conformal mantle cloaks for cylindrical objects using sub-wavelength printed and slotted arrays," *J. Appl. Phys.* **112**, 034907 (2012).

[30]   P. Y. Chen, J. Soric, Y. R. Padooru, H. M. Bernety, A. B. Yakovlev, and A Alù, "Nanostructured graphene metasurface for tunable terahertz cloaking," *New J. Phys.* **15**, 123029 (2013).
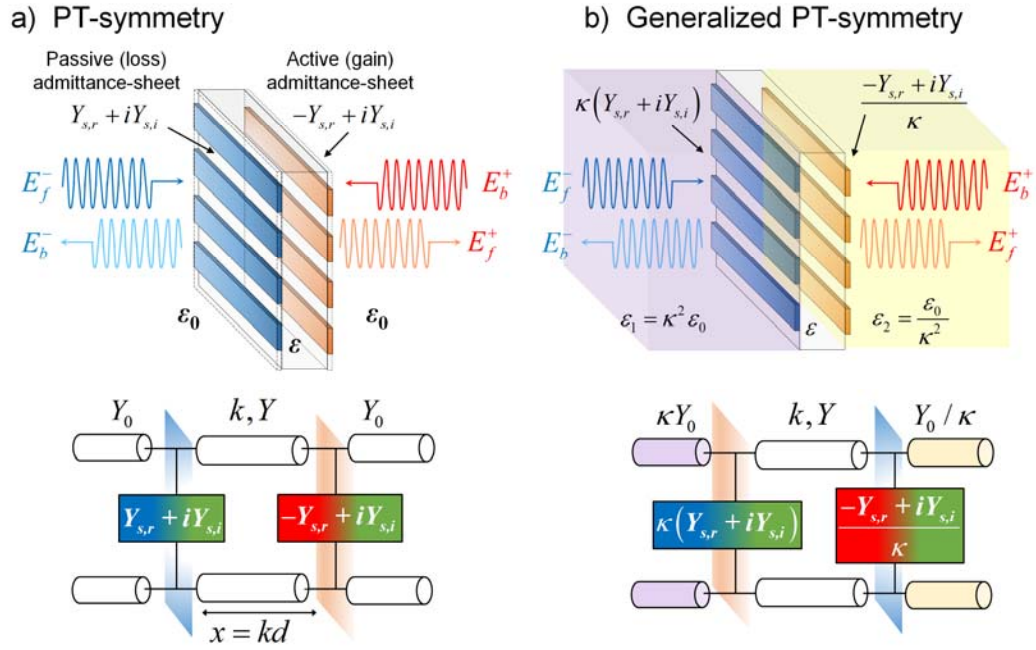
FIGURES

Figure 1 Schematics for (a) the PT-symmetric and (b) the generalized PT (gPT)-symmetric optical structures (top) comprising paired gain and loss components, and their corresponding transmission-line network model (bottom). Provided that the structured gain and loss media have subwavelength thickness and unit cells, their optical behaviors can be described by a surface admittance (or surface impedance). In the gPT-symmetric system, if the scaling coefficient $\kappa \neq 1$, the balance between gain and loss parameters, as a weaker constraint of PT-symmetry, can be broken, while the scattering properties remain the same at the design frequency.
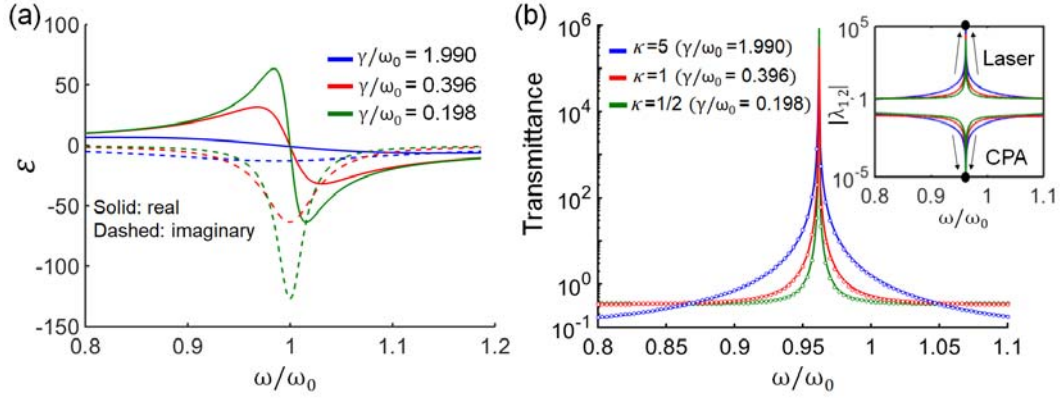
Figure 2 (a) Real (solid) and imaginary (dashed) parts of permittivity of active gain media with different linewidths of amplification γ. (b) Transmittance spectra of gPT-symmetric optical structures in Fig. 1b, of which the amplifying metasurface made of gain media in (a); dashed lines and symbols represent analytical and full-wave simulation results, respectively. By varying the scaling coefficient κ, the CPA-laser point with eigenvalues going to zero and infinite (inset) can be achieved at the design frequency $\omega_D = 0.962\omega_0$, regardless of the gain strength at ω_D. Here, we consider only one excitation, and, thus, only the lasing mode can be observed.
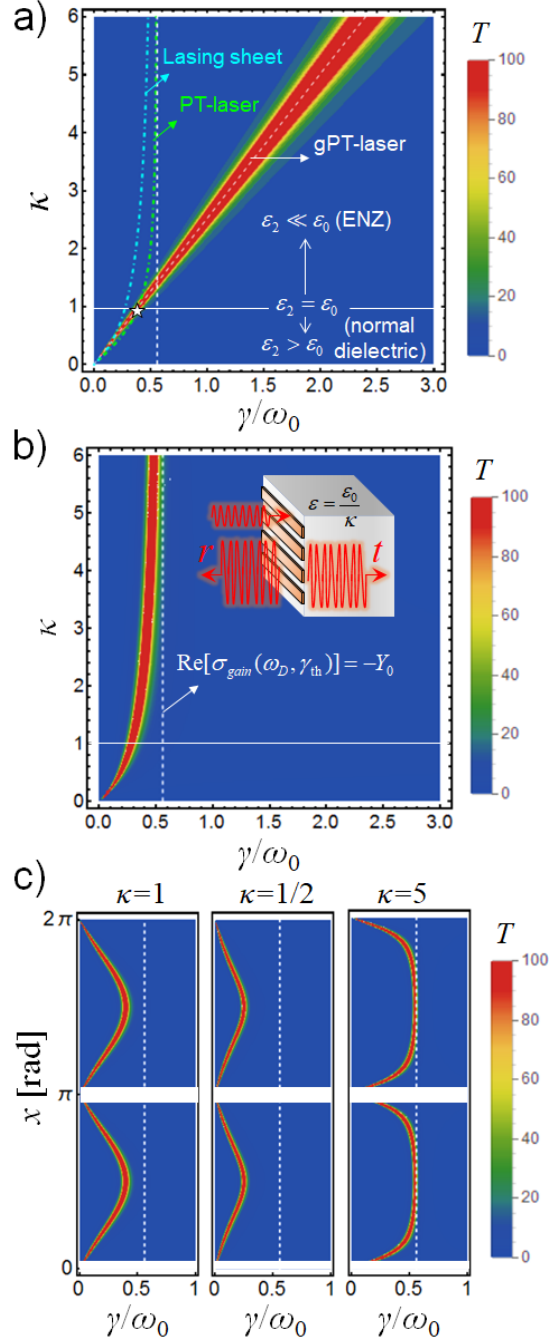
Figure 3 Contours of Transmittance as functions of γ and κ for the gPT-symmetric optical system in Fig. 1(b); here, the locus of optimal (γ, κ) sets, giving the lasing effect, for an individual active metasurface (inset of Fig. 3(b)), PT- and gPT-symmetric optical systems are presented for comparison. For a large γ, corresponding to a weak resonant gain, the lasing effect can only be achieved

with the gPT-symmetric metasurfaces. If $\kappa = 1$, the system would degenerate into the common PT-symmetric setup, as highlighted with a star. (b) is similar to (a), but for an individual active metasurface, showing an upper bound for lasing in terms of γ. Contours of Transmittance as functions of γ and x (electrical length between amplifying and attenuating surfaces) for the PT-symmetric optical system in Fig. 1(a), varying the dielectric permittivity of spacer $\varepsilon = \varepsilon_0 / \kappa^2$. In this case, a physical bound similar to an individual active metasurface in (b) is still obtained.
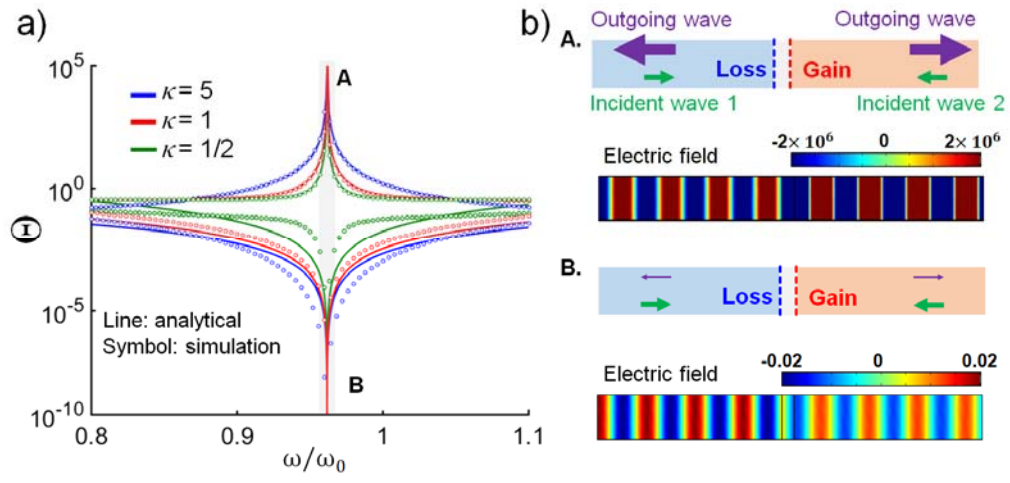
Figure 4 (a) Output coefficient versus frequency for CPA-laser devices based on gPT-symmetric metasurfaces, which are designed using different scaling coefficients; here, lasing and CPA modes are excited by single and two coherent incident waves. (b) Snapshots of electric fields for the gPT-symmetric CPA-laser in (a) ($\kappa = 1$), operated in the lasing mode (top) and the CPA mode (bottom).